Modeling NMR Chemical Shift: A Survey of Density Functional Theory Approaches for Calculating Tensor Properties

Travis H. Sefzik, Domenic Turco, and Robbie J. Iuliucci*
Washington and Jefferson College, Washington, Pennsylvania 15301

Julio C. Facelli
Center for High Performance Computing, University of Utah, Utah 84112
Received: September 29, 2004; In Final Form: November 23, 2004

The NMR chemical shift, a six-parameter tensor property, is highly sensitive to the position of the atoms in a molecule. To extract structural parameters from chemical shifts, one must rely on theoretical models. Therefore, a high quality group of shift tensors that serve as benchmarks to test the validity of these models is warranted and necessary to highlight existing computational limitations. Here, a set of 102 ^{13}C chemical-shift tensors measured in single crystals, from a series of aromatic and saccharide molecules for which neutron diffraction data are available, is used to survey models based on the density functional (DFT) and Hartree−Fock (HF) theories. The quality of the models is assessed by their least-squares linear regression parameters. It is observed that in general DFT outperforms restricted HF theory. For instance, Becke's three-parameter exchange method and mpw1pw91 generally provide the best predicted shieldings for this group of tensors. However, this performance is not universal, as none of the DFT functionals can predict the saccharide tensors better than HF theory. Both the orientations of the principal axis system and the magnitude of the shielding were compared using the chemical-shift distance to evaluate the quality of the calculated individual tensor components in units of ppm. Systematic shortcomings in the prediction of the principal components were observed, but the theory predicts the corresponding isotropic value more accurately. This is because these systematic errors cancel, thereby indicating that the theoretical assessment of shielding predictions based on the isotropic shift should be avoided.

Introduction

The sensitivity of the chemical shift on electronic structure is well established.[1] While this sensitivity may be unrivalled, the chemical shift has an elusive dependence on the molecular structure and, therefore, spectroscopists must rely on theory to ascertain the valuable structural information encoded within the shift. Now that accurate quantum mechanical calculations can be achieved with modest computational resources, quantum mechanical predictions of chemical shielding are routinely used to describe the shift in terms of structural parameters. Conversely, the intimate structure-shielding relationship endorses modeling the chemical shift as a means to develop theoretical methodologies. For these reasons, numerous studies of shielding calculations can be found in the literature.[2] The extensive use of these methodologies makes it greatly important to establish the reliability limits of common methods used to calculate chemical shieldings, but these limits ought to be based on the best experimental measurements available.

The chemical shift is a tensor quantity whose parameters can be readily measured to a high degree of accuracy, 0.75−1.5 ppm for ^{13}C nuclei, in the solid state. This accuracy is improved to <0.5 ppm for single-crystal NMR data.[3] In comparison, the quantum mechanical theory has a reliability for carbon nuclei on the 3−6 ppm level.[1] While this accuracy may be impressive, calculated shieldings still limit the confidence of many conclusions derived from NMR chemical-shift data.[4] Solid-state NMR data may be complemented with high quality diffraction data, which provide the structural parameters for theoretical models. Hence, it is possible to simultaneously have high quality chemical-shift data and an accurate corresponding molecular structure of a system for modeling purposes.[5,6]

It is advantageous to consider the complete chemical-shift tensor when judging theory, because the directional properties of the tensor are associated with the nuclei's three-dimensional electronic environment. This orientational information may shed light on the failings of a theoretical model masked by the isotropic averaging. Therefore, a more stringent test is obtained by modeling the tensor parameters as opposed to limiting the judgment to the isotropic value. The latter may lead to the accidental cancellation of erroneous features predicted by the theory. In addition, the tensor components span a larger range of values than their isotropic values. The increased range of measured shift values and the additional number of measured parameters significantly improve the fitting statistics, thus reducing the uncertainty in the fitting parameters.

Density functional theory (DFT) has gained considerable popularity due to its computational efficiency and is therefore promising for quantum mechanical calculations of complex systems. However, the semiempirical character of DFT challenges its development and a universal acceptance is still desired.[7] The common approach to test shielding calculations[8−17] has been limited to small tests on simple molecules where rotvibrational corrected experimental chemical shifts are known. Clearly, the expansion of theoretical studies to a larger class of molecules is warranted. However, an appropriate test group has not been established. The sheer number of shifts published in the literature and the high spectral resolution makes liquid-phase experimental data attractive. However, this test group brings

* Corresponding author. E-mail: riuliucci@washjeff.edu.

10.1021/jp0455780 CCC: $30.25
Published on Web 01/25/2005

the experimental conditions into question because the temperature and solvent dependences on the shifts are well-known. Further, confidence in the nuclear coordinates used in the model becomes questionable because they too are commonly provided by theory.

Although sufficient data of chemical-shift tensors exist,[18] tensor data have yet to be fully utilized for testing DFT methodologies. Here, we demonstrate the value of using the complete chemical-shift tensor by comparing the performance of the Hartree−Fock method for calculating chemical shieldings with several density functional theory approaches that have been proposed. We limit the scope of the experimental shift values to the highly precise single-crystal ^{13}C tensor data acquired at the University of Utah over the years. To best mimic the solid-phase structure of the shift data, neutron diffraction data are used here to determine the nuclear coordinates in order to avoid uncertainties in the calculations due to the poor resolution of the hydrogen atom positions observed in X-ray studies.[5] At this point in time, intermolecular effects and vibrational correction to molecular geometries are handled indirectly as their influence is reflected in the observed diffraction coordinates. Regardless of this limitation in the model, their absence does not overshadow the merits of using tensor data to judge theoretical models as demonstrated here.

Theoretical Background

Chemical Shielding. Chemical shielding refers to the phenomenon associated with the secondary magnetic field created by the induced motions of the electrons surrounding the nuclei when in the presence of an applied magnetic field. The energy of a magnetic moment, μ, in a magnetic field, **B**, is

$$E = -\mu\cdot(1-\sigma)\mathbf{B} \tag{1}$$

where the shielding, σ, is the differential resonance shift due to the induced motion of the electrons. The chemical shielding is characterized by a real three-by-three Cartesian matrix, which can be decomposed into a single scalar term, three antisymmetric pseudovector components, and five components corresponding to a symmetric tensor.[19] Only the single scalar and the five symmetric tensor elements can be observed in the normal NMR spectra of solids. For brevity, these six values are usually referred to as the shielding tensor:

$$\begin{bmatrix} \sigma_{xx} & \sigma_{xy} & \sigma_{zx} \\ \sigma_{xy} & \sigma_{yy} & \sigma_{yz} \\ \sigma_{zx} & \sigma_{yz} & \sigma_{zz} \end{bmatrix} \tag{2}$$

that can be obtained by averaging the off-diagonal values of the complete tensor.

NMR experiments do not allow the direct measurement of the chemical shielding, but rather, the variation in resonance frequencies of different nuclei provides the measurement of their relative shieldings called the chemical shift. These experimentally measured shifts, δ^e, obey the same tensor properties of the chemical shielding. The calculated shielding, $\sigma^c_{ij,}$ and experimental shift, δ^e_{ij}, elements have a one-to-one correspondence given by

$$\sigma^c_{ij} = m\delta^e_{ij} + K_{ij}\sigma_{ref} \tag{3}$$

where the proportionality constant, m, is equal to -1 and the offset value, σ_{ref}, corresponds to the isotropic shielding of the reference compound. The offset value is only added to diagonal elements as expressed in eq 3 by the use of the Kronecker delta, K_{ij}. The isotropic shielding of the reference compound is either estimated from gas-phase measurements or assumed from calculations.[20] The linear relationship between the chemical shift and shielding given by eq 3 can be transformed into a linear least-squares regression for the comparison of the calculated shieldings to the measured shifts by making both m and σ_{ref} adjustable fitting parameters. The total degrees of freedom become six times the number of tensors subtracting two to account for the proportionality constant and the offset value. Since the uncertainties in the experimental measured shift frequencies are much less than the ability to calculate shielding values, the experimental tensor elements will be set as the independent variable.

The nonuniform addition of an offset value to the Cartesian tensor elements in eq 3 presents a complication when comparing two tensors quantitatively, and all six elements cannot be equally judged.[21] This complexity can be handled in two ways. The six elements can be separated into two sets of three principal values and three Euler angles describing their spatial orientation. With this approach, the principal values and angles are analyzed separately. Alternatively, the tensor can be transformed into the icosahedral representation, which is orthogonal in six dimensions, eliminating the differential treatment of the diagonal and nondiagonal elements as with the Cartesian representation.

The six icosahedral shielding parameters are related to the Cartesian representation by the following transformations:

$$\begin{aligned}
\sigma_1 &= a^2\sigma_{xx} + b^2\sigma_{yy} - ab\sigma_{xy} \\
\sigma_2 &= a^2\sigma_{xx} + b^2\sigma_{yy} + ab\sigma_{xy} \\
\sigma_3 &= a^2\sigma_{yy} + b^2\sigma_{zz} - ab\sigma_{yz} \\
\sigma_4 &= a^2\sigma_{yy} + b^2\sigma_{zz} + ab\sigma_{yz} \\
\sigma_5 &= a^2\sigma_{zz} + b^2\sigma_{xx} - ab\sigma_{zx} \\
\sigma_6 &= a^2\sigma_{zz} + b^2\sigma_{xx} + ab\sigma_{zx}
\end{aligned} \tag{4}$$

where the normalization constants a and b are

$$a = \left(\frac{5+\sqrt{5}}{10}\right)^{1/2} \tag{4a}$$

$$b = \left(\frac{5-\sqrt{5}}{10}\right)^{1/2} \tag{4b}$$

respectively. The orthogonality of the icosahedral representation implies that each icosahedral component is scaled identically and each element has the same offset value added when transforming between relative (shift) and absolute (shielding) scales

$$\sigma^c_i = \hat{m}\delta^e_i + \hat{\sigma}_{ref} \tag{5}$$

where the numerical index, i, denotes the six icosahedral parameters. All six icosahedral parameters contribute equally to the isotropic value.

$$\sigma_{isotropic} = \frac{1}{6}\left(\sum_{i=1}^{6}\sigma_i\right) \tag{6}$$

The linear correlation between calculated shieldings and measured shift values allows the model chemistries used in the calculations to be evaluated using the scatter in the fit and deviations from an ideal slope as a measurement of their success.

Due to the large uncertainty in the determination of the absolute chemical shieldings of reference compounds, it is unwise to use the comparison of the linear regression intercept with the absolute shielding of the reference as a valid quality of the theoretical model. In this paper, we have determined the scatter of the fit by a root-mean-square deviation (rmsd)

$$\mathrm{rmsd} = \sqrt{\frac{\sum_{i=1}^{n}(\sigma^{c}_{i} - (\hat{m}\delta^{e}_{i} + \hat{\sigma}_{\mathrm{ref}}))^2}{n-2}} \tag{7}$$

where n is the total number of tensor elements, i.e., 6 times the number of complete tensors.

Shielding Distance. The difference between two tensors can conveniently be described with a single scalar geometric distance.[21] In the icosahedral representation, the shielding distance, d, is the square root of the average difference between the six orthogonal tensor parameters:

$$d^2_{\mathrm{full}} = \frac{1}{6}\sum_{i=1}^{6}(\sigma_i - \sigma'_i)^2 \tag{8}$$

where σ_i and σ'_i are the ith icosahedral tensor components of the two tensors being compared. The shielding distance only becomes meaningful when the two sets of tensors are given in the same reference scale (i.e., relative shift or absolute shielding) and in the same reference frame (i.e., molecular or crystallographic frame). All the tensors used in this paper are in the crystal frame that was also used in the calculations. The shielding distance, eq 8, reproduces the rmsd, eq 7, but it is useful to identify systematic deficiencies in the model chemistries used in the shielding calculations by examining individual components of the tensor such as the isotropic value, the individual principal components, or their orientation.

While the three individual principal components of two tensors can be compared directly, the squared shielding distance for the three components in the icosahedral representation is given by

$$\begin{aligned} d^2_{\mathrm{pv}} = {} & \frac{1}{15}[3(\sigma_{11} - \sigma'_{11})^2 + 3(\sigma_{22} - \sigma'_{22})^2 + 3(\sigma_{33} - \sigma'_{33})^2 + \\ & 2(\sigma_{11} - \sigma'_{11})(\sigma_{22} - \sigma'_{22}) + 2(\sigma_{11} - \sigma'_{11})(\sigma_{22} - \sigma'_{22}) + \\ & 2(\sigma_{22} - \sigma'_{22})(\sigma_{33} - \sigma'_{33}) + 2(\sigma_{33} - \sigma'_{33})(\sigma_{11} - \sigma'_{11})] \end{aligned} \tag{9}$$

d^2_{pv} is derived by diagonalizing the two Cartesian tensors and neglecting the differences in the Euler angles. In other words, the principal axis systems of the two tensors are assumed identical. Given d^2 and d^2_{pv}, the distance accounting for their different orientations can be determined by subtracting the principal value distance squared from the full distance squared:

$$d^2_{\mathrm{orient}} = d^2_{\mathrm{full}} - d^2_{\mathrm{pv}} \tag{10}$$

This allows for the orientation of the tensors to be quantified in units of ppm. A rms can be determined for the set of shielding distances

$$\mathrm{rms} = \sqrt{\frac{\sum_{i=1}^{n} d^2_i}{n}} \tag{11}$$

TABLE 1: Theory—Exchange and Correlation Functionals

symbol[a]	exchange functional	correlation functional
rhf	Hartree−Fock approach	none
hfb	Becke's 1988 functional	none
hfs	Slater	none
blyp	Becke's 1988 functional	Lee, Yang, and Parr
b3lyp	Becke's three-parameter hybrid	Lee, Yang, and Parr
b3p86	Becke's three-parameter hybrid	Perdew's 1986 gradient corrected
bvwn	Becke's 1988 functional	Vosko, Wilk, and Nussair
svwn	Slater	Vosko, Wilk, and Nussair
mpw1pw91	modified Perdew−Wang	Perdew−Wang 1991

[a] See ref 22 for details.

where d^2_i can be either d^2, d^2_{pv}, or d^2_{orient} or the squared distance for any of the three individual principal components for the ith tensor.

Computational Details

All chemical shielding calculations were performed using the Gaussian quantum mechanical software package.[22] The level of theory or model chemistries were specified by a combination of quantum mechanical method and basis set. The double and triple correlation consistent basis sets of Dunning, cc-pvdz and cc-pvtz, were used in all the calculations.[23] The basis sets were selected for this study following the work by Botto et al.[24] who demonstrated their utility in the calculation of NMR chemical shieldings. Eight standard density functional approaches along with the restricted Hartree−Fock approach were used to model the chemical shielding data. The different exchange and correlation functionals used in the DFT calculations are given in Table 1. These 18 model chemistries are listed in Table 2. The gauge including (invariant) atomic orbital (GIAO) method[25] was used in all the NMR shielding tensor calculations performed here. The statistical analysis of the data was done using programs written in the framework of the MathWorks MatLab software package.[26]

By the various quantum mechanical methods, 102 complete ^{13}C chemical-shift tensors from 15 molecules (naphthalene,[27,28] acenaphthlene,[29,30] triphenylene,[31,32] sucrose,[33,34] methyl-D-mannopyranoside,[35,36] methyl-D-galactopyranoside,[35,37] methyl-D-glucopyranoside,[35,38] methyl-D-xylopyranoside,[35,39] methyl-D-fructopyranose,[40,41] methyl-D-xylopyranose,[40,42] methyl-L-sorbopyranose,[40,43] methyl-L-rhamnose,[44,45] and pentaerythritol[46,47]) were modeled. The molecules were selected because there are data on their full ^{13}C chemical-shift tensors and accurate atomic coordinates from neutron diffraction data. To ensure equal quality of the NMR data, only single-crystal studies with tensor elements measured with a precision below 0.5 ppm were included in the study. The NMR data and neutron diffraction structures were taken from the literature as indicated above. The data analyzed included all 102 carbon tensors in those molecules. Subsets of the 35 sp^2 carbon tensors from the aromatic molecules and the 65 oxygenated sp^3 carbons (i.e., alcohol, ether, methoxy, acetal, ketal, or hemiacetal carbon) from the saccharide molecules were also considered separately.

Results and Discussion

Linear Regression. The overall quality of the linear correlation between the experimental carbon shifts and the calculated shieldings is very impressive. The least-squares parameters (scatter, slope, and intercept) for the 18 model chemistries are presented in Table 2. The scatter estimates the model's inconsistency to describe the shielding of chemically similar nuclei that contain subtle differences in solid-phase structure, while the slope reflects systematic flaws of the methodologies.

TABLE 2: Least-Squares Regression of Model Chemistries with Tensor Test Group

		all carbons (102)			all saccharide (65)			aromatic (35)		
method	basis	rmsd	slope[a]	intercept[b]	rmsd	slope[c]	intercept[b]	rmsd	slope[a]	intercept[b]
rhf	cc-pvdz	5.35	−1.069	211.7	4.14	−0.956	205.2	4.91	−1.043	205.4
rhf	cc-pvtz	5.58	−1.104	204.0	3.73	−0.966	196.0	5.41	−1.078	197.4
hfb	cc-pvdz	5.74	−0.908	180.6	5.02	−1.091	192.5	3.54	−0.905	182.6
hfb	cc-pvtz	5.97	−0.965	171.9	5.08	−1.150	183.7	4.07	−0.969	175.1
hfs	cc-pvdz	5.88	−0.954	187.6	5.38	−1.144	200.1	3.12	−0.944	188.4
hfs	cc-pvtz	5.94	−1.019	177.7	5.49	−1.203	189.7	3.37	−1.015	179.5
blyp	cc-pvdz	5.70	−0.922	181.9	5.05	−1.108	194.0	3.34	−0.916	183.2
blyp	cc-pvtz	5.87	−0.981	172.8	5.03	−1.171	185.0	3.77	−0.982	175.5
b3lyp	cc-pvdz	4.79	−0.966	189.6	4.70	−1.085	197.6	3.32	−0.953	188.7
b3lyp	cc-pvtz	4.78	−1.022	180.8	4.60	−1.133	188.2	3.73	−1.015	180.9
b3p86	cc-pvdz	4.61	−0.972	192.9	4.51	−1.091	201.1	3.13	−0.955	191.2
b3p86	cc-pvtz	4.46	−1.022	184.6	4.31	−1.130	192.0	3.40	−1.011	183.9
bvwn	cc-pvdz	5.46	−0.920	181.2	4.81	−1.099	193.0	3.38	−0.912	182.0
bvwn	cc-pvtz	5.58	−0.975	172.3	4.76	−1.156	184.0	3.76	−0.975	174.7
svwn	cc-pvdz	5.57	−0.967	188.5	4.98	−1.155	201.1	3.18	−0.950	187.9
svwn	cc-pvtz	5.55	−1.030	178.4	4.99	−1.211	190.4	3.38	−1.022	179.2
mpw1pw91	cc-pvdz	4.41	−0.983	194.8	4.42	−1.081	201.8	3.12	−0.964	192.6
mpw1pw91	cc-pvtz	5.14	−1.036	188.2	5.58	−1.112	193.8	3.40	−1.017	185.5

[a] The uncertainty in the slope is 0.002 shielding ppm/shift ppm. [b] The uncertainty in the intercept is 0.2 ppm. [c] The uncertainty in the slope is 0.003 shielding ppm/shift ppm.

TABLE 3: *F* Probability Distribution for the Least-Squares rmsd

	all	saccharide	aromatic
degrees of freedom	610	388	208
ratio for 5% probabilty	1.14	1.18	1.26
lowest rmsd (ppm)	4.41	3.73	3.12
cutoff rmsd (ppm)	4.71	4.06	3.50

The scatter, recorded as a root-mean-square deviation, has units of ppm. Since the ^{13}C chemical-shift values span 220 ppm, a rmsd of 4.5−6.3 ppm is only a relative error of 2.0−2.7%. The ideal proportionality constant, −1, can be reproduced to 2% by three of the DFT methods. The ability of the theory to predict the shift is best exemplified graphically in Figure 1, where the Hartree−Fock and DFT model chemistries with the smallest rmsd are plotted for all 102 tensors, that is, the 65 saccharide tensors and the 35 aromatic tensors. With a reliability better then 3%, one can readily justify the use of quantum mechanical calculations to assign complete experimental tensor data to nuclear positions in simple molecules. However, when presented with partial tensor data (i.e., the principal values obtained by powered samples), better accuracy is necessary to ubiquitously assign the data.[4]

An *F*-test was used to evaluate the rmsd values in order to compare statistically the model chemistries. In Table 3, we report the minimum rmsd values that are required to make their differences not significantly different at the 5% probability level. The variance of the models is represented by the squared rmsd. The *F*-ratio that corresponds to a 5% probability is determined, allowing one to estimate the 5% cutoff rmsd value for the three groups of tensors. It has been found that no single model chemistry statistically outperforms all of the others. For instance when considering all 102 tensors, the b3p86 functional is equivalent to the mpw1pw91/cc-pvdz model. Ten of the 18 models are found to be equivalent to mpw1pw91/cc-pvdz for the aromatic group of tensors. All of the acceptable models are of the DFT type, and each of them represents a significant improvement over the Hartree−Fock approach. It is commonly argued that the lack of electron correlation prevents the HF approach from predicting the shielding of aromatic carbon tensors.[19]

The inability of the increased basis set, cc-pvtz, to improve the rmsd may be indicative of the large basis sets required for magnetic properties. The paramagnetic term of the shielding is dependent on the outer electrons, requiring a sizable basis for their description. A convergence of the isotropic shielding of gas-phase molecules has been shown to require larger than triple-ζ.[14] To observe an improvement, one may need to go beyond the triple-ζ basis set.

Components. The individual tensor elements in themselves carry information about the chemical bonding in a molecule. Given their orientational dependence, systematic flaws in the tensor components may shed light on inadequacies of the model. Table 4 lists the chemical shielding distance for all the model chemistries analyzed here. The shielding distance for the full tensor reproduces the rmsd of the linear correlation fit, and no additional information is gained from column one of Table 4.

The proportionality constant in the regression analysis is a good indicator of systematic problems associated with the theory and its ability to describe the electronic structure near a particular type of atomic hybridization, that is, sp^2 carbon, sp^3 carbon, or oxygen substitution effects. The small uncertainty in the slopes, 0.003 ppm shielding/ppm shift or less, compared to the large variation of slopes reported for the different models, 0.01 ppm shielding/ppm shift or more, allows one to derive conclusions about the theory based on deviations from the ideal slope. A slope > -1 indicates that the model chemistry overpredicts the shielding, while a slope < -1 suggests an underestimation of the shielding magnitude. The Hartree−Fock level adequately describes the saccharide shielding range but overestimates the aromatic values by 5−9%. The slope here may be compensating for the lack of electron correlation in the HF approach. The overestimation of the shielding by the DFT methodologies is significantly high, 10−20%. This suggests an inherent systematic deficiency with DFT to describe the effect of oxygen substitution or that the hydrogen bonding effects, not included in these models, may be playing a decisive role on the saccharide carbon tensors. It is interesting to observe that the slope increases with the larger basis set for every case regardless of the theory or carbon type. However, to make conclusions about this trend, further studies with larger basis sets are necessary.

The magnitude of the chemical shielding is captured by the principal components of the tensor. The combined shielding distance for all three principal values, d_{pv}, obtained by eq 11 shows the ability of the theory to predict the overall shielding magnitude. Once more, the accuracy of the theory is impressive;

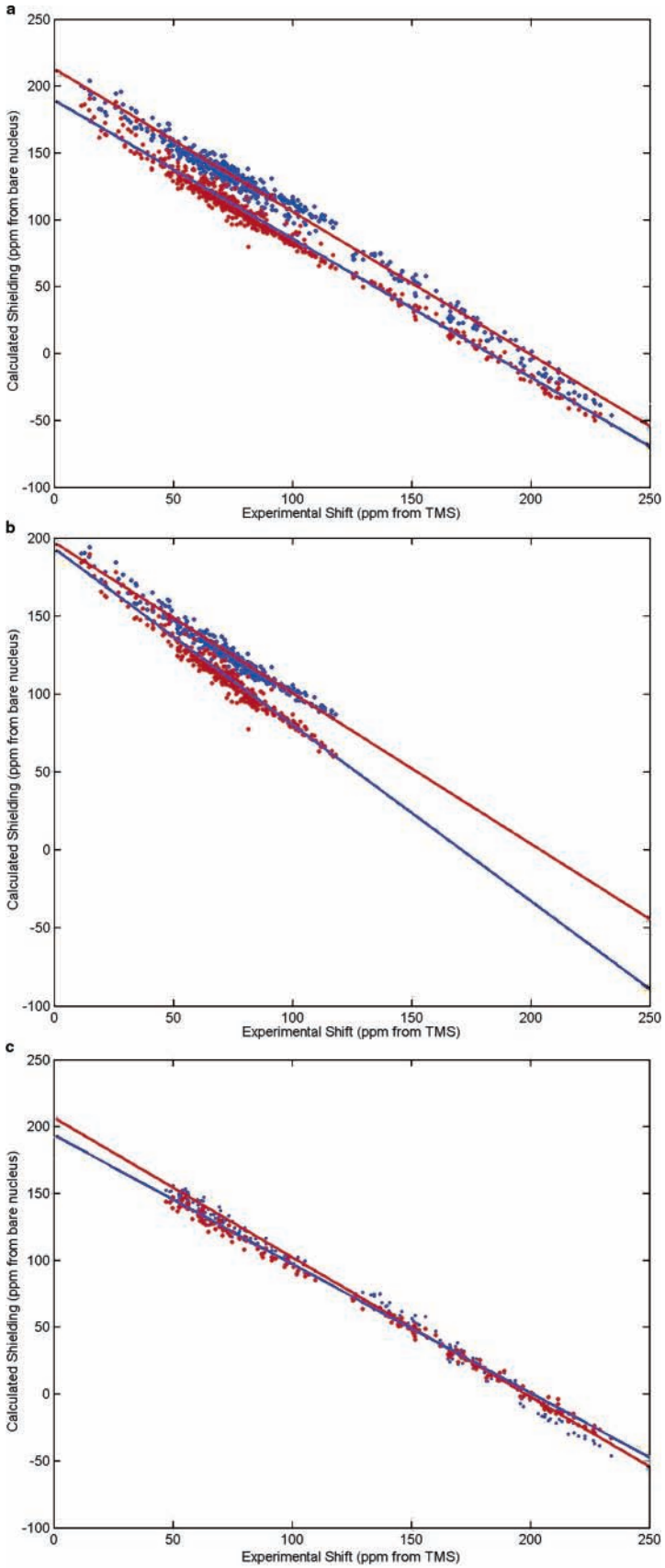

Figure 1. (a) Linear correlation between calculated chemical shielding and experimental shift values. All 102 tensors are considered. The model chemistries plotted are the lowest rmsd HF method, rhf/cc-pvdz (blue dots with red line), and the DFT method, mpw1pw91/cc-pvtz (red dots with blue line). The tensor parameters are in the icosahedral representation. (b) Linear correlation between calculated chemical shielding and experimental shift values when only the 65 saccharide tensors are considered. The model chemistries plotted are the lowest rmsd HF method, rhf/cc-pvtz (blue dots with red line) and DFT method, b3p86/cc-pvtz (red dots with blue line). The tensor parameters are in the icosahedral representation. (c) Linear correlation between calculated chemical shielding and experimental shift values when only the 35 aromatic tensors are considered. The model chemistries plotted are the lowest rmsd HF method, rhf/cc-pvdz (blue dots with red line), and the DFT method, mpw1pw91/cc-pvtz (red dots with blue line). The tensor parameters are in the icosahedral representation.

TABLE 4: Chemical-Shift Distance of Model Chemistries with the Tensor Test Group[a]

method	basis	full tensor	principal	isotropic	σ_{11}	σ_{22}	σ_{33}	orientation
			All Tensors					
rhf	cc-pvdz	5.35	4.28	3.80	6.74	4.82	6.49	2.29
rhf	cc-pvtz	5.58	4.59	3.80	7.60	5.10	6.86	2.25
hfb	cc-pvdz	5.74	4.41	4.38	6.00	5.06	6.85	2.65
hfb	cc-pvtz	5.97	4.60	4.38	5.61	5.93	7.25	2.86
hfs	cc-pvdz	5.88	4.35	4.46	5.77	4.21	7.67	2.83
hfs	cc-pvtz	5.94	4.35	4.35	5.14	4.40	8.01	3.05
blyp	cc-pvdz	5.70	4.31	4.35	6.06	4.61	6.89	2.67
blyp	cc-pvtz	5.87	4.49	4.35	5.66	5.24	7.26	2.86
b3lyp	cc-pvdz	4.79	3.36	3.47	4.54	3.99	5.78	2.52
b3lyp	cc-pvtz	4.78	3.31	3.24	4.06	4.41	5.86	2.67
b3p86	cc-pvdz	4.61	3.20	3.25	4.63	3.45	5.54	2.53
b3p86	cc-pvtz	4.46	3.00	2.93	3.98	3.52	5.48	2.64
bvwn	cc-pvdz	5.46	4.10	4.09	6.18	4.36	6.25	2.63
bvwn	cc-pvtz	5.58	4.24	4.05	5.75	4.91	6.60	2.81
svwn	cc-pvdz	5.57	4.10	4.14	6.00	3.77	7.07	2.71
svwn	cc-pvtz	5.55	4.02	4.00	5.35	3.66	7.35	2.91
mpw1pw91	cc-pvdz	4.41	2.96	3.04	4.30	3.29	5.29	2.50
mpw1pw91	cc-pvtz	5.14	3.41	3.92	4.41	4.85	5.89	2.62
		5.36	**3.95**	**3.89**	**5.43**	**4.42**	**6.58**	**2.67**
			All Saccharide					
rhf	cc-pvdz	4.14	2.76	3.06	4.01	2.61	4.30	2.45
rhf	cc-pvtz	3.73	2.36	2.46	3.48	2.14	4.03	2.43
hfb	cc-pvdz	5.02	3.43	3.78	4.50	3.80	5.98	2.70
hfb	cc-pvtz	5.08	3.37	3.65	4.03	3.51	6.32	2.95
hfs	cc-pvdz	5.38	3.76	3.89	4.27	4.03	6.84	2.99
hfs	cc-pvtz	5.49	3.67	3.79	3.92	3.74	7.23	3.26
blyp	cc-pvdz	5.05	3.45	3.80	4.46	3.90	5.93	2.72
blyp	cc-pvtz	5.03	3.30	3.62	4.01	3.42	6.19	2.94
b3lyp	cc-pvdz	4.70	3.18	3.55	4.26	3.42	5.41	2.59
b3lyp	cc-pvtz	4.60	2.96	3.28	3.78	2.94	5.54	2.76
b3p86	cc-pvdz	4.51	3.01	3.33	4.16	3.31	4.83	2.61
b3p86	cc-pvtz	4.31	2.65	2.96	3.56	2.71	4.84	2.74
bvwn	cc-pvdz	4.81	3.23	3.61	4.61	3.65	5.15	2.67
bvwn	cc-pvtz	4.76	3.02	3.42	4.03	3.21	5.40	2.87
svwn	cc-pvdz	4.98	3.43	3.67	4.26	3.78	5.93	2.78
svwn	cc-pvtz	4.99	3.23	3.50	3.77	3.32	6.16	3.02
mpw1pw91	cc-pvdz	4.42	2.92	3.24	4.07	3.17	4.69	2.60
mpw1pw91	cc-pvtz	5.58	3.52	4.61	4.66	5.23	5.61	2.76
		4.81	**3.18**	**3.51**	**4.10**	**3.44**	**5.58**	**2.77**
			All Aromatic					
rhf	cc-pvdz	4.91	4.11	1.97	6.48	8.04	4.58	2.17
rhf	cc-pvtz	5.41	4.64	1.93	7.24	9.53	4.74	2.21
hfb	cc-pvdz	3.54	2.79	1.64	3.56	5.03	3.87	1.96
hfb	cc-pvtz	4.07	3.25	1.59	4.18	6.61	4.22	2.12
hfs	cc-pvdz	3.12	2.27	1.54	2.92	2.98	4.02	1.96
hfs	cc-pvtz	3.37	2.51	1.50	3.30	3.40	4.41	2.10
blyp	cc-pvdz	3.34	2.57	1.64	3.32	4.17	3.82	1.95
blyp	cc-pvtz	3.77	2.94	1.61	3.84	5.39	4.23	2.10
b3lyp	cc-pvdz	3.32	2.58	1.61	3.64	4.18	3.76	1.87
b3lyp	cc-pvtz	3.73	2.95	1.56	4.21	5.42	4.11	1.98
b3p86	cc-pvdz	3.13	2.39	1.56	3.34	3.30	3.87	1.84
b3p86	cc-pvtz	3.40	2.63	1.49	3.80	4.01	4.19	1.95
bvwn	cc-pvdz	3.38	2.62	1.73	3.37	4.27	3.82	1.94
bvwn	cc-pvtz	3.76	2.94	1.66	3.85	5.29	4.24	2.09
svwn	cc-pvdz	3.18	2.36	1.56	2.94	3.18	4.24	1.94
svwn	cc-pvtz	3.38	2.50	1.57	3.20	3.01	4.82	2.07
mpw1pw91	cc-pvdz	3.12	2.39	1.53	3.44	3.29	3.78	1.84
mpw1pw91	cc-pvtz	3.40	2.65	1.48	3.93	4.15	4.04	1.93
		3.63	**2.84**	**1.62**	**3.92**	**4.74**	**4.15**	**2.00**

[a] The chemical-shift distance is reported as a rms in units of ppm.

the average d_{pv} rms is <4 ppm. Overall, b3p86/cc-pvtz and mpw1pw91/cc-pvdz give the lowest d_{pv} rmsd. Attention should be given to mpw1pw91/cc-pvdz because of the smaller deviation from unity slope and the smaller number of basis functions associated with cc-pvdz. Again, the above rmsd trends for the different models to predict the shielding are reproduced in the shielding magnitude.

Since the principal value distance assumes identical principal axis systems for the compared tensors, the square root of the difference between d^2 and d^2_{pv} reflects the discrepancies in the tensor orientation. This orientational distance, d_{orient}, allows the assessment of the ability of the theory to predict the principal axis system in units of ppm. From Table 4, one sees that the theory can predict the orientation equally if not better than the magnitude of the shielding. This trend appears independent of the model. Furthermore, the variation in d_{orient} between the different models is smaller than the variations observed in the prediction of the magnitude. Therefore, the failing of a model to predict the orientation is not proportional to its inability to predict the magnitude. For the aromatic tensors, the rms of d_{orient} is significantly less than the one for the magnitude. This can be explained by the fact that the associated ring currents dictate that σ_{33} is perpendicular to the molecular plane.[5,27,29,31] In comparison, the principal axis system of the sp^3 saccharide tensors is less constrained. There is only a modest improvement of the theory to reproduce the orientation compared to the magnitude, 10% on average. For the saccharide tensors, the Hartree−Fock approach provides the best prediction of the tensor orientation.

The examination of the three individual principal components reveals some systematic problems with the theory. For the saccharide molecules, σ_{22} systematically has the smallest rms distance, while σ_{33} has the largest. On average, the differences are >2 ppm. Conversely, σ_{22} is typically the worst principal value predicted for the aromatic tensors. This pattern is not as consistent throughout the model chemistries as it is with the saccharide tensors. For the aromatic tensors, σ_{22} is the shielding perpendicular to the carbon−hydrogen bond and may be indicative of problems associated with the position or motion of the hydrogen atom.

Isotropic Shielding. When examining the shielding of gas- or liquid-phase molecules that incorporate spatial averaging, comparison of theories is limited to the isotropic shift values. To highlight the potential to obtain misleading results, we examine isotropic rmsd's here. The values presented are considerably smaller than those found by others, which is primarily a consequence of using a linear model as opposed to the absolute differences.[17] Furthermore, the improvement can be attributed to the careful selection of compounds for this study that included only those with high quality diffraction structures as well as NMR data.

Since systematic errors are suspected in the theoretical predictions of the individual principal values, accurate isotropic predictions can only be observed accidentally. This is particularly evident for the HF method. d_{iso} for rhf/cc-pvtz is a third of d_{pv}, suggesting that the calculations are capable of reproducing the isotropic shift very accurately. However, this accuracy comes as an oversimplification and this fallacy can be revealed by considering error propagation. The uncertainty, E, in the isotropic value can be estimated by propagating the errors from the three principal components

$$E_{iso} = \left[\left(\frac{\partial\sigma_{iso}}{\partial\sigma_{11}}\right)^2 E^2_{11} + \left(\frac{\partial\sigma_{iso}}{\partial\sigma_2}\right)^2 E^2_{22} + \left(\frac{\partial\sigma_{iso}}{\partial\sigma_{33}}\right)^2 E^2_{33}\right]^{1/2} \quad (12)$$

where the uncertainty in the principal components can be estimated from the rms distance, d_{ii}. The partial derivative of the isotropic shift with respect to each of the principal components is a constant, $^1/_3$. Assuming no correlation between the uncertainties in the principal components, the uncertainty in the isotropic value for the rhf/cc-pvtz model should exceed 4.3 ppm, a value approximately equal to d_{pv}. The rmsd for the

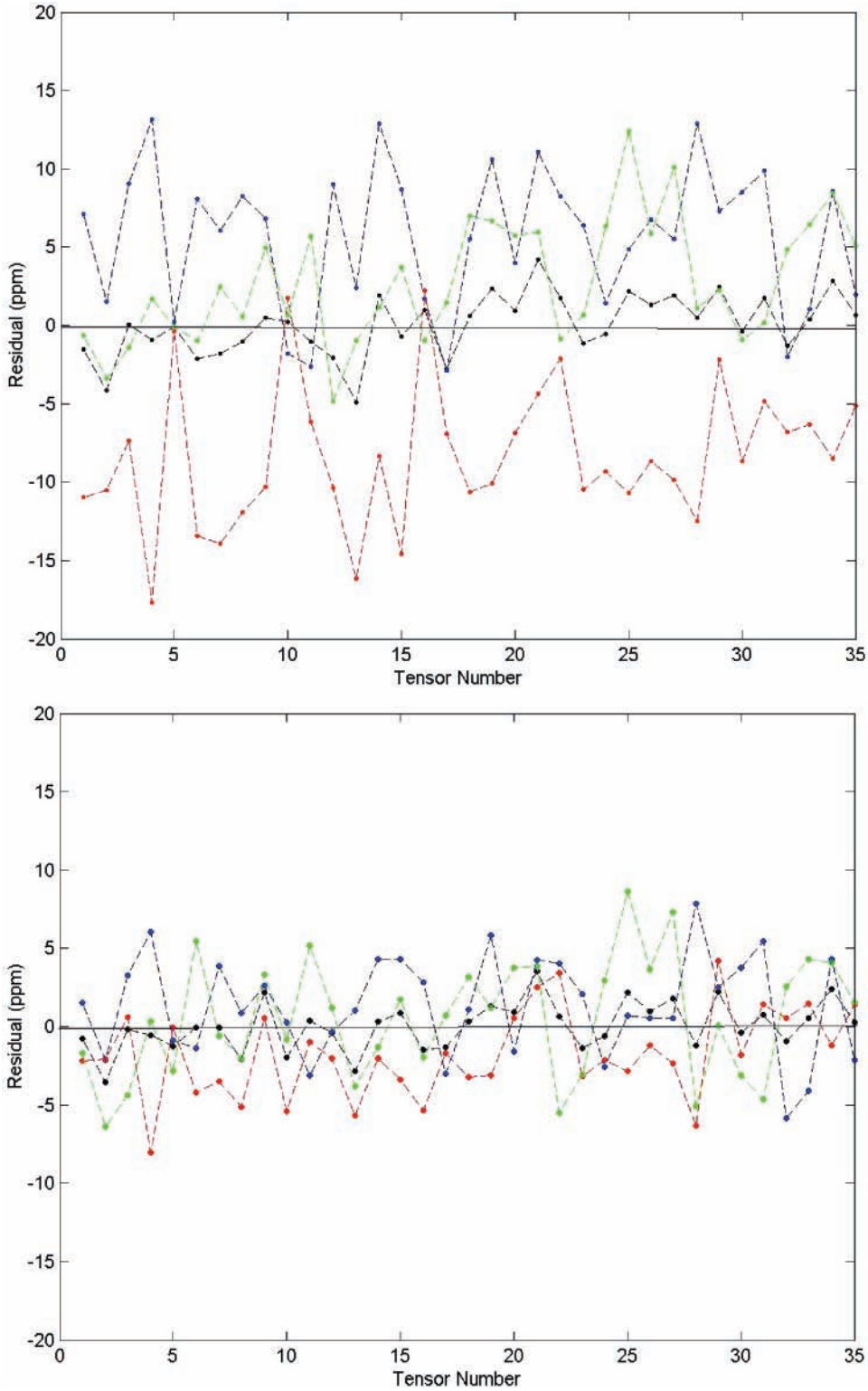

Figure 2. Residuals between the predicted shielding and experimental shift principal components for rhf/cc-pvtz (top) and mwp1pw91/cc-pvdz (bottom). See text for details.

isotropic value is drastically underestimated. Once more, d_{pv} is a better indicator for a method to predict the magnitude of the shielding.

By examining the residual difference between the calculated shielding and the experimentally observed shielding, the cancellation effect for obtaining the artificially good isotropic values becomes self-evident. Figure 2 contains the residuals of the three principal values (blue, σ_{11}; red, σ_{22}; green, σ_{33}) as well as for the isotropic value (black) for rhf/cc-pvtz (top) and mpw1pw91/cc-pvdz (bottom) of the aromatic tensors. Not only are the deviations of the principal components large, 9.53 ppm for σ_{22} of rhf/cc-pvtz, but they are also biased. The errors in one principal component, σ_{22}, for the aromatic carbon are counterbalanced by the errors in the other two components, $\sigma_{11}$and σ_{33}. The resulting isotropic value is predicted artificially accurate, as seen by the small deviation from zero for each tensor. For the DFT method, the principal components deviate significantly less and do not appear as biased. The mpw1pw91/cc-pvdz residuals of the individual components are shown to be more random and less systematically predicted than with the HF method.

Conclusions

Accurate calculations of the nuclear magnetic shielding potentially allows for a direct interpretation of the resonant shift in terms of molecular structure. To achieve this goal, reliable model chemistries must be identified. The computational demands of large molecular systems make density functional theory an attractive alternative to pure ab initio approaches. Hence, the development of a means to assess these model chemistries is necessary. Here, an analysis based on the complete tensor combined with quality diffraction coordinates is proposed as a test group of moderate size molecules.

For carbon chemical shifts, the current level of theory to predict the shift is at the 3−6 ppm range.[3] Again, the results here show current DFT methods are comparable and in many cases outperform HF. In particular, Becke's three-parameter exchange method as well as mpw1pw91 tends to perform well for the groups of tensors considered here. However, the diminished ability for these functionals to predict the saccharide carbon tensors fails to show universal consistency. New hybrid and generalized gradient approximation functionals, designed for shielding calculations, have recently been proposed,[48−50] and it will be important to test how well these functionals can predict the shielding tensor used here.

The results using the complete tensor to assess model chemistries emphasized current systematic problems. The deviation from ideal slopes was at times alarmingly high, 10−20%. The trend for the triple-ζ basis to increase the slope without improving the rmsd was also observed. The availability of the complete tensor allows for one to critique the principal axis system in units of ppm. The orientational dependence of principal components may be used to spatially explain the failings of the theory. Moreover, the tendency of the methods to systematically predict principal components erroneously can result in an artificially accurate isotropic value, limiting the use of gas- or liquid-phase chemical-shift data.

Acknowledgment. Computer resources for this project were partially provided by the Center for High Performance Computing at the University of Utah. This work was supported in part by Los Alamos National Laboratory. We would like to thank Don Alderman for his discussions about the expression to obtain the chemical-shift distance for the principal axis system. Also, suggestions and comments on this manuscript made by David M. Grant were appreciated.

References and Notes

(1) Facelli, J. C., De Dios, A. C., Eds. *Modeling NMR Chemical Shifts: Gaining Insights into Structure and Environment*, Proceedings of the Second International Symposium held at the 216th National Meeting of the American Chemical Society, Boston, MA, Aug 23−26, 1998; American Chemical Society: Washington, DC, 1999 (ACS Symposium Series 732).

(2) Jameson, C. J.; De Dios, A. C. Theoretical and Physical Aspects of Nuclear Shielding. *A Specialist Periodical Report: Nuclear Magnetic Resonance*; Royal Society of Chemistry: London, 2005; Vol. 34, Chapter 2.

(3) Orendt, A. M. Chemical shifts measurements in solids. In *Encyclopedia of Nuclear Magnetic Resonance*; Grant, D. M., Harris, R. K., Eds.; London: John Wiley & Sons, 1996; pp 1282−1297.

(4) Iuliucci, R. J.; Clawson, J.; Hu, J.; Solum, M. S.; Barich, D. H.; Grant, D. M.; Taylor, C. M. *Solid State Nucl. Magn. Reson.* **2003**, *24*, 23.

(5) Grant, D. M.; Liu, F.; Iuliucci, R. J.; Phung, C. G.; Facelli, J. C.; Alderman, D. W. *Acta Crystallogr., Sect. B* **1995**, *51*, 540.

(6) Helgaker, T.; Jaszunski, M.; Ruud, K. *Chem. Rev.* **1999**, *99*, 293.

(7) Jameson, C. J.; De Dios, A. C. Theoretical and Physical Aspects of Nuclear Shielding. *A Specialist Periodical Report: Nuclear Magnetic Resonance*; Royal Society of Chemistry: London, 2001; Vol. 30, p 46.

(8) Gauss, J.; Stanton, J. F. *J Chem. Phys.* **1996**, *104* (7), 2574.

(9) Handy, N. C.; Tozer, D. J. *Mol. Phys.* **1998**, *94* (4), 707.

(10) Wilson, P. J.; Amos R. D.; Handy, N. C. *Mol. Phys.* **1999**, *97* (6), 757.

(11) Bienati, M.; Adamo, C.; Barone, V. *Chem. Phys. Lett*. **1999**, *311*, 69.

(12) Wilson, P. J.; Tozer, D. J. *Chem. Phys. Lett.* **2001**, *337*, 341.

(13) Wilson, P. J.; Tozer, D. J. *J. Chem. Phys.* **2002**, *116* (23), 10139.

(14) Kupka, T.; Ruscic, B.; Botto, R. E. *J. Phys. Chem. A* **2002**, *106*, 10396.

(15) Fadda, E.; Casida, M. E.; Salahub, D. R. *J. Chem. Phys.* **2003**, *118* (15), 6756.

(16) Keal, T. W.; Tozer, D. J.; Helgaker, T. *Chem. Phys. Lett.* **2004**, *391*, 374−379.

(17) Cheeseman, J. R.; Trucks, G. W.; Keith, T. A.; Frisch, M. J. *J. Chem. Phys.* **1996**, *104*, 5497.

(18) Duncan, T. M. *Principal Components of Chemical Shift Tensors: A Compilation*, 2nd ed.; Cornell University: Ithaca, NY, 1997.

(19) Facelli, J. C. *Encyclopedia of Nuclear Magnetic Resonance*; Grant, D. M., Harris, R. K., Eds.; London: John Wiley & Sons, 2002; Vol. 9, p 323.

(20) Jameson, C. J. *ACS Symp. Ser*. **1999**, *732*, 1.

(21) Alderman, D. W.; Sherwood, M. H.; Grant, D. M. *J. Magn. Reson., Ser. A* **1993**, *101*, 188.

(22) Frisch, M. J.; Trucks, G. W.; Schlegel, H. B.; Scuseria, G. E.; Robb, M. A.; Cheeseman, J. R.; Montgomery, J. A., Jr.; Vreven, T.; Kudin, K. N.; Burant, J. C.; Millam, J. M.; Iyengar, S. S.; Tomasi, J.; Barone, V.; Mennucci, B.; Cossi, M.; Scalmani, G.; Rega, N.; Petersson, G. A.; Nakatsuji, H.; Hada, M.; Ehara, M.; Toyota, K.; Fukuda, R.; Hasegawa, J.; Ishida, M.; Nakajima, T.; Honda, Y.; Kitao, O.; Nakai, H.; Klene, M.; Li, X.; Knox, J. E.; Hratchian, H. P.; Cross, J. B.; Adamo, C.; Jaramillo, J.; Gomperts, R.; Stratmann, R. E.; Yazyev, O.; Austin, A. J.; Cammi, R.; Pomelli, C.; Ochterski, J. W.; Ayala, P. Y.; Morokuma, K.; Voth, G. A.; Salvador, P.; Dannenberg, J. J.; Zakrzewski, V. G.; Dapprich, S.; Daniels, A. D.; Strain, M. C.; Farkas, O.; Malick, D. K.; Rabuck, A. D.; Raghavachari, K.; Foresman, J. B.; Ortiz, J. V.; Cui, Q.; Baboul, A. G.; Clifford, S.; Cioslowski, J.; Stefanov, B. B.; Liu, G.; Liashenko, A.; Piskorz, P.; Komaromi, I.; Martin, R. L.; Fox, D. J.; Keith, T.; Al-Laham, M. A.; Peng, C. Y.; Nanayakkara, A.; Challacombe, M.; Gill, P. M. W.; Johnson, B.; Chen, W.; Wong, M. W.; Gonzalez, C.; Pople, J. A. *Gaussian 03*; Gaussian, Inc.: Pittsburgh, PA, 2003.

(23) Dunning, T. H., Jr. *J. Chem. Phys.* **1989**, *90*, 1007.

(24) Kupka, T.; Ruscic, B.; Botto, R. E. *Solid State Nucl. Magn. Reson.* **2003**, *23*, 145−167.

(25) Wolinski, K.; Hinton, J. F.; Pulay, P. *J. Am. Chem. Soc.* **1990**, *112*, 8251.

(26) *Matlab*, Release 12.1; The Mathworks, Inc.: Natick, MA 2001.

(27) Sherwood, M. H.; Facelli, J. C.; Alderman, D. W.; Grant, D. M. *J. Am. Chem. Soc.* **1991**, *113*, 750.

(28) Pawley, G. S.; Yeats, E. *A. Acta Crystallogr., Sect. B* **1969**, *25*, 2009.

(29) Iuliucci, R. J.; Facelli, J. C.; Alderman, D. W.; Grant, D. M. *J. Am. Chem. Soc.* **1995**, *117*, 2336.

(30) Hazell, A. C.; Hazell, R. G.; Noerskov-Lauritsen, L.; Briant, C. E.; Jones, D. W. *Acta Crystallogr., Sect. C* **1986**, *42*, 690.

(31) Iuliucci, R. J.; Phung, C. G.; Facelli, J. C.; Grant, D. M. *J. Am. Chem. Soc.* **1998**, *120* (36), 9305.

(32) Ferraris, G.; Jones, D. W.; Yerkess, J. *Z. Kristallogr*. **1973**, *138*, 113.

(33) Sherwood, M. H.; Alderman, D. W.; Grant, D. M. *J. Magn. Reson., Ser. A* **1993**, *104*, 132.

(34) Brown, G. M.; Levy, H. A. *Acta Crystallogr., Sect. B* **1973**, *29*, 790.

(35) Liu, F.; Phung, C. G.; Alderman, D. W.; Grant, D. M. *J. Am. Chem. Soc.* **1996**, *118*, 10629.

(36) Takagi, S.; Jeffrey, G. A. *Acta Crystallogr., Sect. B* **1979**, *35*, 902.

(37) Jeffrey, G. A.; McMullan, R. K.; Takagi, S. *Acta Crystallogr., Sect. B* **1977**, *33*, 728.

(38) Jeffrey, G. A.; Takagi, S. *Acta Crystallogr., Sect. B* **1977**, *33*, 738.

(39) Takagi, S.; Jeffrey, G. A. *Acta Crystallogr., Sect. B* **1977**, *33*, 3033.

(40) Liu, F.; Phung, C. G.; Alderman, D. W.; Grant, D. M. *J. Magn. Reson., Ser. A* **1996**, *120*, 231.

(41) Takagi, S.; Jeffrey, G. *A. Acta Crystallogr., Sect. B* **1977**, *33*, 3510.

(42) Jeffrey, G. A.; Robbins, A.; McMullan, R. K.; Takagi, S. *Acta Crystallogr., Sect. B* **1980**, *36*, 373.

(43) Nordenson, S.; Takagi, S.; Jeffrey, G. A. *Acta Crystallogr., Sect. B* **1979**, *35*, 1005.

(44) Liu, F.; Phung, C. G.; Alderman, D. W.; Grant, D. M. *J. Magn. Reson., Ser. A* **1996**, *120*, 242.

(45) Takagi, S.; Jeffrey, G. A. *Acta Crystallogr., Sect. B* **1978**, *34*, 2551.

(46) Liu, F.; Orendt, A. M.; Alderman, D. W.; Grant, D. M. *J. Am. Chem. Soc.* **1997**, *119*, 8981.

(47) Semmingsen, D. *Acta Chem. Scand.* **1988**, *A42*, 279.

(48) Keal, T. W.; Tozer, D. J. *J. Chem. Phys.* **2003**, *119*, 3015.

(49) Keal, T. W.; Tozer, D. J. *J. Chem. Phys.* **2004**, *121*, 5654.

(50) Teale, A. M.; Tozer, D. J. *Chem. Phys. Lett.* **2004**, *383*, 109.